International Journal of Nanomedicine

Dovepress
open access to scientific and medical research

Open Access Full Text Article

ORIGINAL RESEARCH

Preparation and properties of poly(vinyl alcohol)/chitosan blend bionanocomposites reinforced with cellulose nanocrystals/ZnO-Ag multifunctional nanosized filler

This article was published in the following Dove Press journal:
International Journal of Nanomedicine
23 April 2014
Number of times this article has been viewed

Susan Azizi[1]
Mansor Bin Ahmad[1]
Mohd Zobir Hussein[1]
Nor Azowa Ibrahim[1]
Farideh Namvar[2,3]

[1]Department of Chemistry, Faculty of Science, [2]Institute of Tropical Forestry and Forest Products, University Putra Malaysia, Selangor, Malaysia; [3]Mashhad Branch, Islamic Azad University, Mashhad, Iran

Abstract: A series of novel bionanocomposites were cast using different contents of zinc oxide-silver nanoparticles (ZnO-AgNPs) stabilized by cellulose nanocrystals (CNC) as multifunctional nanosized fillers in poly(vinyl alcohol)/chitosan (PVA/Cs) matrices. The morphological structure, mechanical properties, ultraviolet-visible absorption, and antimicrobial properties of the prepared films were investigated as a function of their CNC/ZnO-AgNP content and compared with PVA/chitosan/CNC bionanocomposite films. X-ray diffraction and field emission scanning electron microscopic analyses showed that the CNC/ZnO-AgNPs were homogeneously dispersed in the PVA/Cs matrix and the crystallinity increased with increasing nanosized filler content. Compared with pure PVA/Cs, the tensile strength and modulus in the films increased from 0.055 to 0.205 GPa and from 0.395 to 1.20 GPa, respectively. Ultraviolet and visible light can be efficiently absorbed by incorporating ZnO-AgNPs into a PVA/Cs matrix, suggesting that these bionanocomposite films show good visibility and ultraviolet-shielding effects. The bionanocomposite films had excellent antimicrobial properties, killing both Gram-negative *Salmonella choleraesuis* and Gram-positive *Staphylococcus aureus*. The enhanced physical properties achieved by incorporating CNC/ZnO-AgNPs could be beneficial in various applications.

Keywords: multifunctional nanofiller, bionanocomposite, cellulose nanocrystals, antimicrobial properties, poly(vinyl alcohol)/chitosan blend

Introduction

In the past decade, cellulose nanocrystals (CNC) have attracted much attention as biomass reinforcement in host biopolymers for developing new nanocomposite materials. CNC are typically rod-formed monocrystals, 2–20 nm in diameter, from tens to hundreds of nanometers in length, and extracted after acid hydrolysis of cellulose.[1,2] CNC as a reinforcing phase have several advantages over other types of nanosized fillers, including a high aspect ratio, low density, outstanding mechanical properties (138 GPa of Young's modulus and 1.7 GPa of tensile strength), renewability, and biocompatibility.[3,4] It has been found that a low volume fraction of monofunctional nanosized fillers only improves a small number of properties of host polymers.[5,6] This feature limits the performance of a polymer nanocomposite. In order to fabricate nanocomposite materials with enhanced properties, mixtures of various nanosized fillers in host polymers could open up new opportunities for preparation of nanocomposites with high performance applications. Inorganic nanoparticles with good chemical and physical properties are

Correspondence: Susan Azizi
Department of Chemistry, Faculty of Science, Universiti Putra Malaysia, 43400 UPM Serdang, Selangor, Malaysia
Email azisusan@gmail.com

submit your manuscript | www.dovepress.com
Dovepress
http://dx.doi.org/10.2147/IJN.S60274

important nanosized fillers that have been effectively used in the functionalization of polymer materials.[7] However, formation of aggregated or agglomerated inorganic nanoparticles will considerably reduce their applicability.[7] One of the successful approaches used to prevent aggregation and improve the dispersion of inorganic nanoparticles has been synthesis of nanoparticles in the presence of surfactants or polymeric ligands.[8] Cellulose-based nanomaterials have been widely used as templates, scaffolds, and carriers to synthesize inorganic nanoparticles.[9–16] Considering the functional properties of cellulose nanocrystals and inorganic nanoparticles, the resulting CNC/inorganic nanoparticle composites – by creating a network structure, improving crystallinity, and interacting with the matrix – can offer a good reinforcing effect in blending with polymer bases. Homogenous dispersion of nanosized fillers in polymer matrices is an important factor affecting the functional properties of polymer nanocomposites. The hydrophilic surface of CNC allows appropriate blending with water-based host polymer matrices.[17] This effect can provide good dispersion of inorganic nanoparticles in a hydrophilic polymer base. Poly(vinyl alcohol) (PVA) is a water-soluble synthetic polymer, is nontoxic, and has good physical and chemical properties.[18] PVA has been used in many biomaterial applications.[19] Chitosan (Cs) is an abundant natural biopolymer with excellent film-forming ability and biocompatibility, is nontoxic, and has high mechanical strength.[20] Cs blended with PVA has been reported to have good mechanical and chemical properties because of the specific intermolecular interactions between PVA and Cs, so this combination is being studied widely in the fields of packaging, membrane filtration, dye adsorption, and biomedicine.[21–23] The improved mechanical, ultraviolet-shielding, and antimicrobial properties of PVA/Cs are valuable.

This study investigates the effect of a multifunctional nanosized CNC/zinc oxide-silver nanoparticle (ZnO-AgNP) filler on the functional properties of PVA/Cs matrices using a solution casting method. Given the functional properties of CNC and ZnO-AgNPs, incorporation of such a multifunctional nanosized filler would be expected to improve the mechanical properties, ultraviolet-absorbing ability, and antibacterial activity of polymer blend nanocomposites.

Materials and methods

Materials

All chemicals were of analytical grade and used as received without further purification. Cotton cellulose from filter paper (Q1, Whatman, Maidstone, UK) was supplied by Fisher Scientific (Pittsburgh, PA, USA). Sulfuric acid (95%–98%, reagent grade) was purchased from Scharlau (Barcelona, Spain). Ethanol and sodium hydroxide were provided by Sigma-Aldrich (St Louis, MO, USA). Zinc acetate dehydrate (99%) and silver nitrate (99.98%), used as precursors, were provided by Merck (Darmstadt, Germany). Cs with an 85% degree of deacetylation and an average molecular weight of "345,500" g/mol was obtained from the Malaysian Nuclear Agency (Selangor, Malaysia). PVA with 99% hydrolysis and an average molecular weight of 89.000 g/mol was purchased from Sigma-Aldrich.

Preparation of CNC/ZnO-AgNPs

CNC/ZnO-AgNPs were synthesized using our previously reported method.[24] Briefly, a sample of $Zn(AcO)_2 \cdot 2H_2O$ alcoholic solution (50 mL, 1 mM) was dispersed in a CNC suspension by magnetic stirring. After complete mixing, a sodium hydroxide solution was added dropwise to the mixed solution under continuous stirring at 80°C until a pH >10 was reached. When a milky colored suspension was observed, a sample of aqueous $AgNO_3$ solution with a concentration of 10 wt% (relative to $Zn(AcO)_2 \cdot 2H_2O$) was added to the above suspension with vigorous stirring, and the reaction was continued for 2 hours. The product was collected by centrifugation and careful washing three times with distilled water. The final product was obtained by drying at 100°C for one hour, with complete transformation of the remaining zinc hydroxide to zinc oxide.

Preparation of bionanocomposites

The PVA/Cs blend was prepared as described elsewhere.[25] The CNC/ZnO-AgNPs were then dispersed in a solution of distilled water (100 mL) and ultrasonicated for 30 minutes. The loading level of the CNC/ZnO-AgNP filler (0, 1, 3, 5, or 7 wt%) was based on the amount of PVA/Cs blend. The above suspensions were added to 100 mL of the PVA/Cs under strong stirring for 2 hours at 70°C. The mixtures were cast onto glass Petri dishes and then dried in ambient temperature to obtain the composite films. The dried composite films were roasted at 45°C for 6 hours. Finally, a series of nanocomposite films with a thickness of ~0.2 mm were prepared. A similar protocol was used to prepare a PVA/Cs/CNC bionanocomposite, but the loading level for the CNC filler was 0.5, 0, 1, 3, or 5 wt% based on the amount of PVA/Cs blend.

Characterization

X-ray analysis was carried out using an X'Pert PRO diffractometer (PANalytical, Almelo, the Netherlands). The X-ray beam was nickel-filtered Cu (λ=1.542 A°) and the instrument

was operated at 40 kV and 30 mA. The scanning scope of 2θ was 5°–80° at room temperature. The upper surface and cross-section morphology of the biocomposite film were examined using a JSM-6360LA field emission scanning electron microscope (Philips, Eindhoven, the Netherlands). The specimens were mounted on a metal stub using carbon tape and then gold-coated using a sputter coater. The size and morphology of the ZnO-Ag/CNC were observed using an H-700 transmission electron microscope (TEM, Hitachi, Tokyo, Japan) with an acceleration voltage of 120 kV at room temperature. The sample for TEM was prepared by dropping a sample of the suspension onto a copper grid coated with carbon film. The specimens were then negatively stained with 1% uranyl acetate and allowed to dry at room temperature. The components of the samples were evaluated by energy-dispersive X-ray spectroscopy. The tensile properties of the original polymer blend and bionanocomposites were measured as per ASTM (American Standard Test Method) D 638 test methods, using an Instron 4032 universal testing machine (Instron, Pfungstadt, Germany). The samples were cut into dumbbell shapes by employing a steel template and router cutter (Die BS 6476). Seven specimens were tested, and the average result of the values of five specimens was taken. The optical properties of the samples were investigated using an ultraviolet-visible near infrared spectrophotometer. The samples were placed in a chamber and then scanned in the wavelength range of 200–800 nm at room temperature.

Antibacterial measurements

The samples were evaluated for antibacterial activity against Gram-negative *Salmonella choleraesuis* and Gram-positive *Staphylococcus aureus*. The bacteria were grown overnight in nutrient broth. The bacterial inoculum was standardized to 0.5 MF units, meaning that approximately 10^8 colony-forming units of each bacterium were inoculated onto a plate. The samples had a diameter of 3 mm, and were placed on a plate inoculated with bacteria. The plates were inverted and incubated at 37°C under ultraviolet light for 24 hours, following which the zone of complete inhibition was measured. Three replicate tests were carried out in the same conditions for each sample. The reported inhibition zone values represent the average of all three samples.

Results and discussion

Characterization of CNC/ZnO-AgNPs

A TEM image of CNC/ZnO-Ag deposited from a dilute aqueous suspension is shown in Figure 1A, and indicates spherical ZnO-AgNPs with a narrow size distribution, which were relatively well dispersed within the rod-like shapes of the CNC. The composition of the particles was characterized in detail by energy-dispersive X-ray spectroscopy (Figure 1B). On energy-dispersive X-ray spectroscopy, signals from Zn, O and Ag were observed in most particles, indicating successful combination of the silver nanoparticles with ZnO.[24] The individual particles visible in the image have diameters of approximately 10 nm. On the other hand, the peaks of C and O are attributed to the binding energies of the CNC.

X-ray diffraction

The X-ray diffraction patterns for CNC/ZnO-AgNP powder, PVA/Cs, and PVA/Cs/CNC/ZnO-Ag films are shown in Figure 2. The CNC/ZnO-Ag shows three sets of diffraction peaks corresponding to CNC, ZnO, and AgNPs in the 2θ range of 10°–80°. The PVA/Cs film shows the characteristic pattern of an amorphous phase with the main halo of the

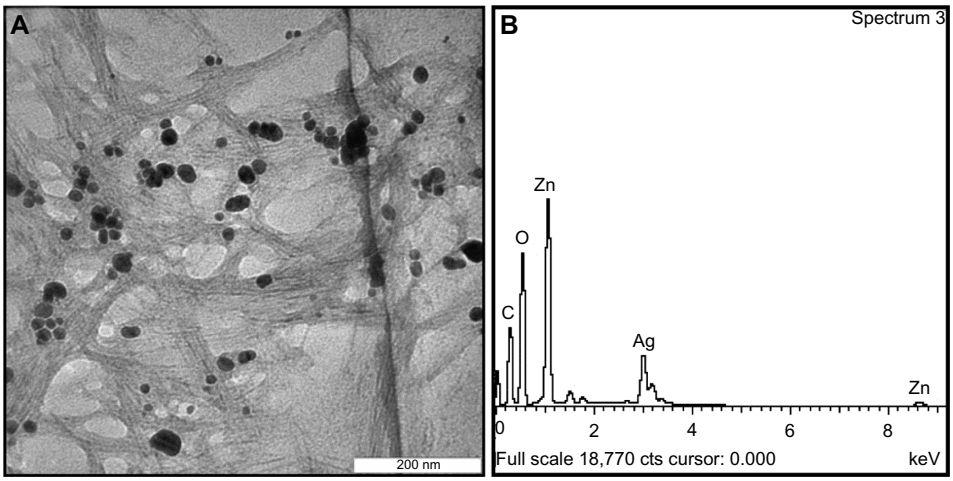

Figure 1 Transmission electron microscopic image (**A**) and energy-dispersive X-ray spectrum (**B**) of CNC/ZnO-AgNPs.
Abbreviations: AgNPs, silver nanoparticles; CNC, cellulose nanocrystals; ZnO, zinc oxide.

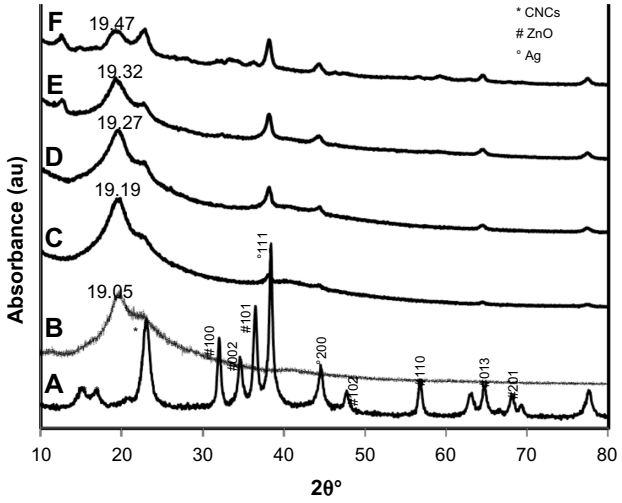

Figure 2 X-ray diffraction patterns for CNC/ZnO-AgNPs (**A**), PVA/Cs blend (**B**), and bionanocomposites from 1.0 to 7.0 wt% (**C**–**F**) nanosized filler loading.
Abbreviations: AgNPs, silver nanoparticles; CNC, cellulose nanocrystals; ZnO, zinc oxide; PVA, poly(vinyl alcohol); Cs, chitosan.

typical peak at a 2θ of 19.05° and another of low intensity at a 2θ of 22.15°.[26] The X-ray diffraction pattern shows the peak of PVA/Cs and several sharp and increased diffraction peaks for PVA/Cs/CNC/ZnO-Ag bionanocomposite films with a relatively high CNC/ZnO-AgNP content. These peaks in the 2θ range of 10°–80° were almost the same as those of the CNC, ZnO, and Ag, although the sharp diffraction peaks increased with increasing CNC/ZnO-Ag content. When a high level of CNC/ZnO-Ag was introduced, the presence of greater numbers of self-agglomerated nanoparticles caused the crystalline character attributed to the CNC, ZnO, and Ag in the bionanocomposite to become more clear. There was neither a new peak nor a peak shift compared with the pure PVA/Cs, indicating that the PVA/Cs/CNC/ZnO-Ag bionanocomposite films all consisted of two phase structures, ie, polymer and nanoparticles. As the CNC/ZnO-AgNP content was increased from 0 to 7.0 wt%, the 2θ value of the peak increased slightly from 19.05° to 19.47°. The Bragg equation was used to calculate the mean intermolecular distance, which decreased from 4.87 Å to 4.69 Å as the CNC/ZnO-AgNP content increased. These results indicate that incorporation of CNC/ZnO-AgNPs did not change the structural uniformity of the matrix polymer blend, but rather improved the molecular ordering in the amorphous polymer blend matrix.

Surface morphology

Figure 3 shows field emission scanning electron micrographs of the upper surfaces (Figure 3A and C) and cross-sections (Figure 3B and D) of PVA/Cs/CNC and PVA/Cs/CNC/ZnO-Ag bionanocomposite films, respectively. The rod-like morphology of the CNC is easily observable in Figure 3A. Homogeneous dispersion of CNC in the PVA/Cs matrix is seen, and indicates good compatibility between the filler and the polymeric blend matrix. The individual CNC visible in the image have diameters of approximately 20 nm and lengths of up to about 250 nm, which are in agreement with values usually reported for wood-derived cellulose nanofibers.[27] In Figure 3C and D, the spherical ZnO-AgNPs and rod-like CNC are uniformly distributed without severe aggregation in the polymer blend matrix. The presence of ZnO-AgNPs was confirmed further by using energy-dispersive X-ray spectroscopy (Figure 3E). The average diameter of the ZnO-AgNPs was approximately 15 nm. The results for crystal shape and size are in agreement with the TEM observations for pristine CNC/ZnO-AgNPs. Some aggregates could be seen at lower magnification, and may have formed during evaporation of water or may have been present in the original suspension.

Mechanical properties

Figure 4A and B show the effect of CNC/ZnO-AgNP content on the mechanical properties of the PVA/Cs/CNC/ZnO-AgNP bionanocomposites. The CNC/ZnO-AgNPs with the PVA/Cs matrix as the nanosized filler showed a notable reinforcing effect. As the nanosized filler content increased, both the tensile strength and Young's modulus increased significantly, but the elongation at break of the composites decreased. When the CNC/ZnO-AgNP content varied from 0 to 5.0 wt%, the tensile yield strength and Young's modulus increased from 0.055 to 0.205 GPa, representing a ~272% enhancement, and the tensile modulus increased from 0.395 to 1.2 GPa, indicating a ~203% increase. This suggests that incorporating CNC/ZnO-AgNPs into the PVA/Cs matrix results in strong interactions between the filler and the matrix, and consequently restricts the motion of the matrix and promotes rigidity.[28] Furthermore, increased crystallinity, which was confirmed by X-ray diffraction analysis, can also enhance mechanical properties.[29] Further addition of CNC/ZnO-AgNPs decreased the tensile strength and modulus, but this still remained higher than that of the original PVA/Cs film. This decrease is due to interparticle interactions, which lead to the creation of weak points in the matrix. On the other hand, the elongation at break gradually decreased from 0 to 7.0 wt% of filler loading, with maximum reduction at 5.0 wt%. The elongation at breaks decreased from 10.3 to 2.1 wt%, representing a ~79% reduction. This phenomenon can be explained by the fact that the rigid filler network structure was created perfectly when the filler content was 5.0 wt%.

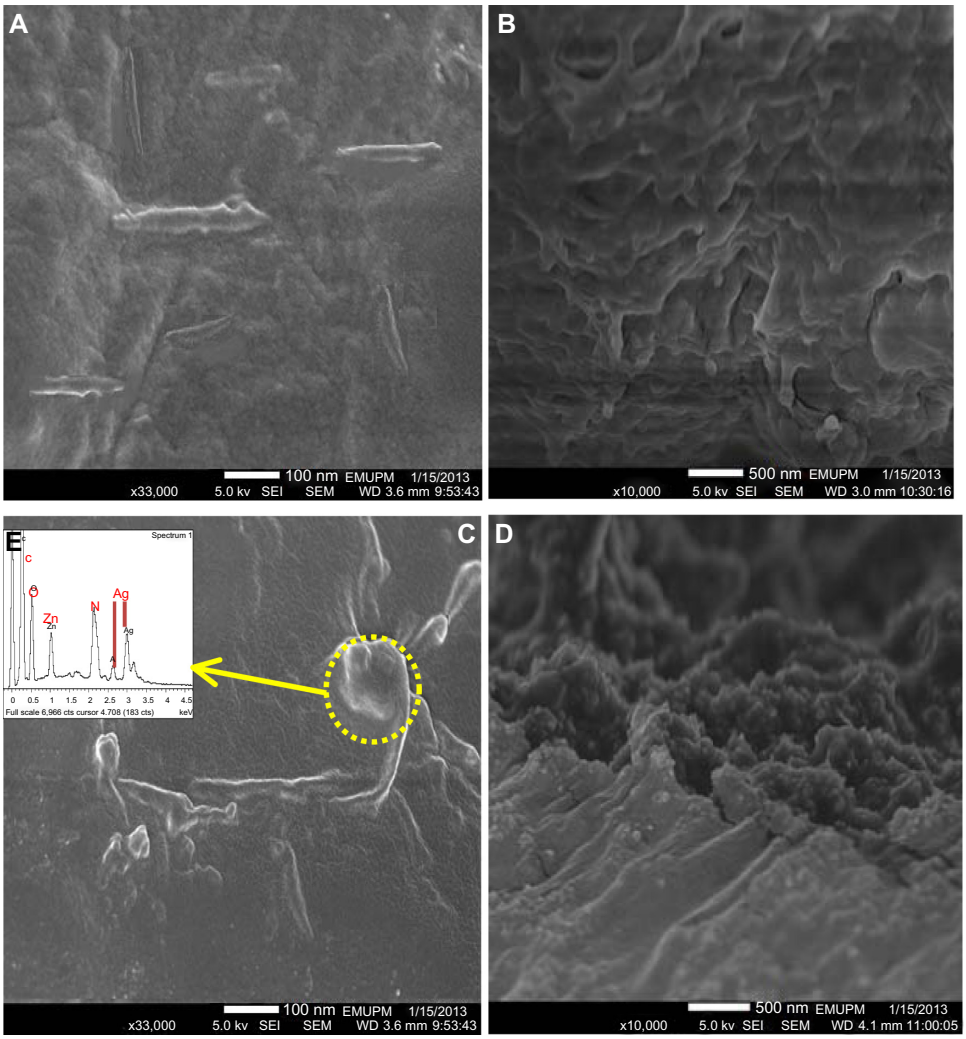

Figure 3 Field emission scanning electron micrographs of upper surfaces (**A** and **C**) and cross-sections (**B** and **D**) of PVA/Cs/CNC 1.0 wt% and PVA/Cs/CNC/ZnO-Ag 5.0 wt% bionanocomposites, respectively. Energy-dispersive X-ray spectrum (**E**) of PVA/Cs/CNC/ZnO-Ag bionanocomposite.
Abbreviations: CNC, cellulose nanocrystals; ZnO, zinc oxide; PVA, poly(vinyl alcohol); Cs, chitosan.

In comparison, the CNC-filled polymer blend bionanocomposites showed a similar trend in tensile properties, but the reinforcing effect of CNC was smaller than that of the CNC/ZnO-AgNPs. The maximum yield strength and Young's modulus were about ~75 and 78%, respectively, at a filler loading of 1.0 wt%. These results indicate that the presence of ZnO-Ag had a positive effect on tensile and Young's modulus values. Meanwhile, the elongation at break of the bionanocomposite films decreased from 0 to 5.0 wt% of CNC loading, with maximum reduction of about ~37% at a filler content of 1.0 wt%.

Ultraviolet absorbance

The optical properties of CNC/ZnO-AgNP, PVA/Cs/CNC, and PVA/Cs/CNC/ZnO-Ag bionanocomposites observed by ultraviolet-visible absorption spectrophotometry are shown in Figure 4. There is no absorption band found in the region of 300–700 nm for the PVA/Cs/CNC bionanocomposites. In comparison, the PVA/Cs/CNC/ZnO-Ag bionanocomposites showed two absorption bands in the ultraviolet and visible regions corresponding to the band gap of the ZnO nanoparticles[30,31] and the surface plasmon resonance of the AgNPs,[32] respectively, and these are clearly evident for CNC/ZnO-AgNPs. On comparison with the CNC/ZnO-AgNPs, the absorption band at ~345 nm has blue shifted to ~335 nm and the absorption peak at ~420 nm has red shifted to ~450 nm for all bionanocomposite films, indicating strong interactions between PVA/Cs and ZnO-AgNPs. Such shifting of the absorption peaks due to the interaction between a polymer matrix and ZnO was been reported by other researchers.[33,34] Otherwise, a band shift can be caused by aggregation of nanoparticles.[35,36] With increasing ZnO-Ag content, the peaks

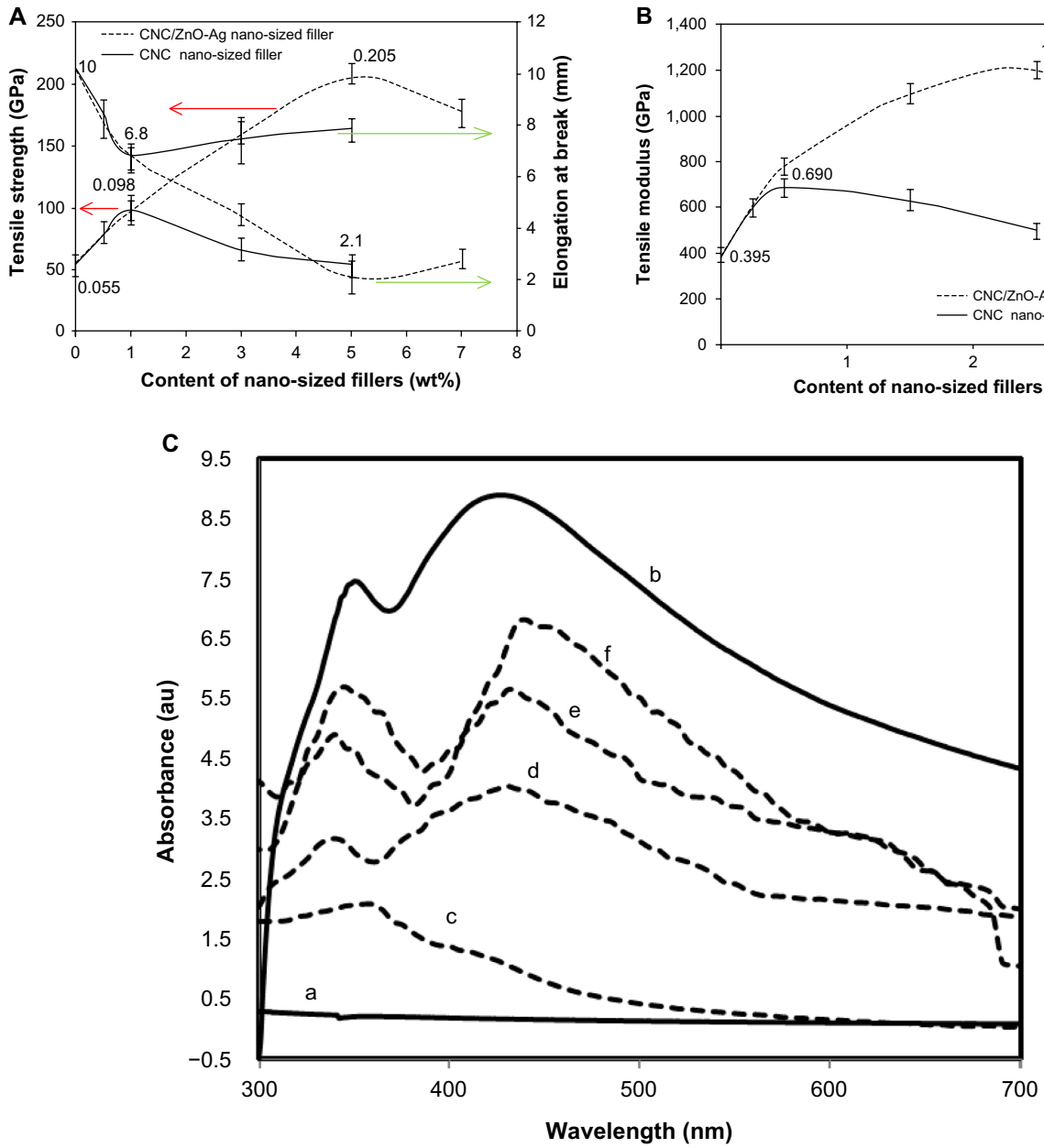

Figure 4 (**A**) Tensile strength and elongation at break of PVA/Cs/CNC/ZnO-Ag and PVA/Cs/CNC bionanocomposites. (**B**) Tensile modulus of PVA/Cs/CNC/ZnO-Ag and PVA/Cs/CNC bionanocomposites. (**C**) Ultraviolet spectra of CNC/ZnO-AgNPs (**a**), PVA/Cs/CNC (**b**), and PVA/Cs/CNC/ZnO-Ag bionanocomposites from 1.0 to 7.0 wt% filler loading (**c**–**f**).
Abbreviations: CNC, cellulose nanocrystals; ZnO, zinc oxide; PVA, poly(vinyl alcohol); Cs, chitosan.

became narrower with increased band intensity, indicating an increase in particle size. Maximum absorption was obtained for the polymer blend with a filler loading of 7.0 wt%. The PVA/Cs/CNC/ZnO-Ag bionanocomposites may successfully protect against ultraviolet and visible light, and could potentially be used as ultraviolet and visible shielding materials.

Antibacterial assessment

The photocatalytic antimicrobial activity of the biocomposite films was examined by measuring the inhibition zones of *S. aureus* and *S. choleraesuis* cells under ultraviolet light, as shown in Figure 5. Table 1 shows the average inhibition zones for all the bionanocomposite samples. In contrast with PVA/Cs/CNC film, the PVA/Cs/CNC/ZnO-Ag bionanocomposites show an inhibition zone against the bacteria. The antibacterial activity of the bionanocomposites can be explained by photocatalysis, metal release, and accumulation of ZnO-AgNPs.[37,38] When ZnO nanoparticles are under light irradiation, electron-hole pairs are generated. The holes split H_2O molecules from ZnO into

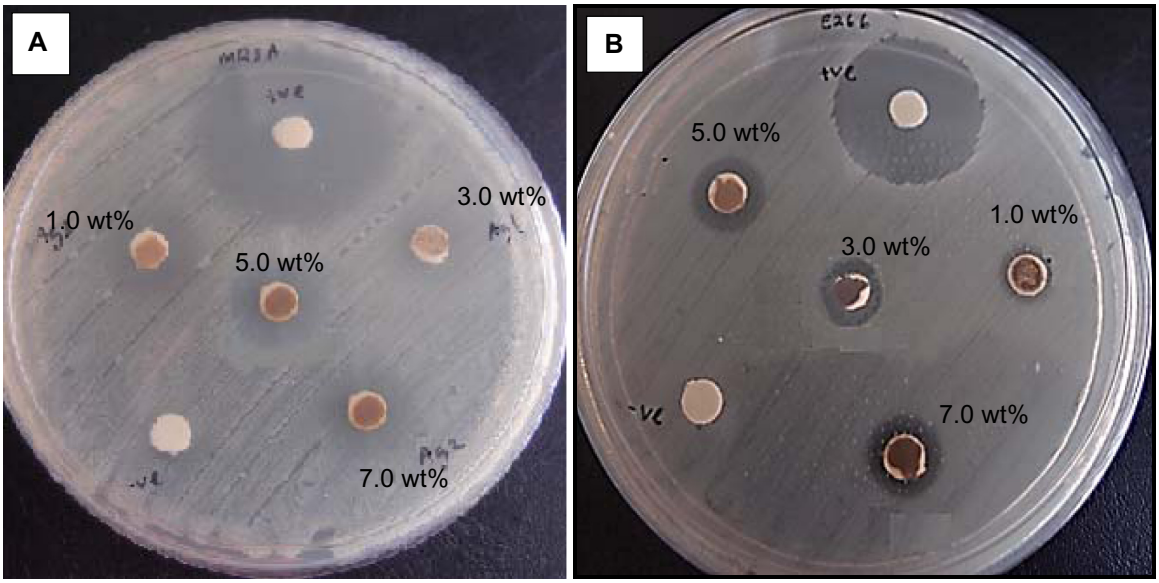

Figure 5 Inhibition zone images of PVA/Cs/CNC/ZnO-Ag bionanocomposites against (**A**) Gram-positive and (**B**) Gram-negative bacteria.
Abbreviations: CNC, cellulose nanocrystals; ZnO, zinc oxide; PVA, poly(vinyl alcohol); Cs, chitosan.

OH^- and H^+. The hole (h^+) reacts with OH^- on the surface of the nanoparticles, generating hydroxyl radicals (OH^+), superoxide anion (O_2^-) radicals, and perhydroxyl radicals (HO_2^+). These highly active free radicals harm bacterial cells, resulting in their decomposition and destruction.[39] On the other hand, the released silver ions may attach to proteins and neutralize them, interact with the microbial membrane to cause structural change and permeability, and interact with microbial nucleic acids to inhibit microbial replication. In addition, accumulation of ZnO-AgNPs in the microbial membrane could result in disorganization of the membrane and internalization into the microbial cell.[40] As shown in Table 1, with increased filler content, the diameter of the inhibition zone gradually increased. A strong antibacterial effect was found for 7.0 wt% PVA/Cs/CNC/ZnO-Ag bionanocomposites. The antibacterial activity of the samples was stronger against *S. aureus* than against *S. choleraesuis*. The difference in antibacterial activity of the bionanocomposites against these two types of bacteria can be related to structural and chemical compositional differences in the cell membrane.[41]

Table 1 Inhibition zone data for PVA/Cs/CNC/ZnO-Ag bionanocomposite films

Filler content wt%	Diameter of zone (mm)	
	Gram-positive	Gram-negative
1.0%	4.6	3.7
3.0%	5.8	4.1
5.0%	7.1	5.6
7.0%	8.3	6.0
0	–	–

Abbreviations: CNC, cellulose nanocrystals; ZnO, zinc oxide; PVA, poly(vinyl alcohol); Cs, chitosan.

Conclusion

A PVA/Cs blend film reinforced with differing CNC/ZnO-AgNP content was prepared using a solution casting method. The strong interaction between the CNC/ZnO-Ag nanosized filler and the PVA/Cs matrix contributed to improvement in the properties of the bionanocomposite. At a low filler loading level (below 5.0 wt%), the CNC/ZnO-Ag bionanocomposites markedly increased the tensile yield strength and Young's modulus of the PVA/Cs/CNC/ZnO-Ag bionanocomposites when compared with the CNC nanosized filler. The ultraviolet results indicate that the PVA/Cs/CNC/ZnO-Ag bionanocomposites can protect against ultraviolet and visible light. Furthermore, PVA/Cs/CNC/ZnO-Ag bionanocomposite films show strong antibacterial activity against *S. choleraesuis* and *S. aureus*. These bionanocomposites have potential applications in medical, textile, packaging, and ultraviolet-shielding materials.

Acknowledgments

The authors are grateful to the staff of the Department of Chemistry, University Putra Malaysia, for their technical assistance, and to the University Putra Malaysia for supporting this work with research grant (RUGS 9199840).

Disclosure

The authors report no conflicts of interest in this work.

References

1. Dufresne A. *Nanocellulose: From Nature to High Performance Tailored Materials*. Boston, MA, USA: Walter De Gruyter Inc.; 2012.
2. Habibi Y, Lucia LA, Rojas OJ. Cellulose nanocrystals: chemistry, self-assembly, and applications. *Chem Rev*. 2010;110:3479–3500.
3. Xu W, Qin ZY, Yu HY, et al. Cellulose nanocrystals as organic nanofillers for transparent polycarbonate films. *J Nanopart Res*. 2013;15:1562–1570.
4. Yu HY, Qin ZY, Liang BL, Liu N, Zhou Z, Chen L. Facile preparation of thermally stable cellulose nanocrystals with high yield of 93% through hydrochloric acid hydrolysis under hydrothermal condition. *J Mater Chem A*. 2013;1:3938–3944.
5. Gao Z, Peng J, Zhong T, Sun J, Wang X, Yue C. Biocompatible elastomer of waterborne polyrethane based on castor oil and polyethylene glycol with cellulose nanocrystals. *Carbohydr Polym*. 2012;87:2068–2075.
6. Bulota M, Tanpichai S, Hughes M, Eichhorn SJ. Micromechanics of TEMPO-oxidized fibrillated cellulose composites. *ACS Appl Mater Interfaces*. 2012;4:331–337.
7. Althues H, Henle J, Kaskel S. Functional inorganic nanofillers for transparent polymers. *Chem Soc Rev*. 2007;36:1454–1465.
8. Ferrando R, Jellinek J, Johnston RL. Nanoalloys: from theory to applications of alloy clusters and nanoparticles. *Chem Rev*. 2008;108:845–910.
9. Cai J, Kimura S, Wada M, Kuga S. Nanoporous cellulose as metal nanoparticles support. *Biomacromolecules*. 2009;10:87–94.
10. Shin Y, Bae I, Arey BW, Exarhos GJ. Facile stabilization of gold-silver alloy nanoparticles on cellulose nanocrystal. *J Phys Chem C*. 2008;112:4844–4848.
11. Shin Y, Bae IT, Arey BW, Exarhos GJ. Simple preparation and stabilization of nickel nanocrystals on cellulose nanocrystal. *Mater Lett*. 2007;61:3215–3217.
12. Shin Y, Exarhos, GJ. Template synthesis of porous titania using cellulose nanocrystals. *Mater Lett*. 2007;61:2594–2597.
13. Liu H, Wang D, Shang S, Song Z. Synthesis and characterization of Ag-Pd alloy nanoparticles/carboxylated cellulose nanocrystals nanocomposites. *Carbohydr Polym*. 2011;83:38–43.
14. Liu H, Wang D, Song Z, Shang S. Preparation of silver nanoparticles on cellulose nanocrystals and the application in electrochemical detection of DNA hybridization. *Cellulose*. 2011;18:67–74.
15. Padalkar S, Capadona JR, Rowan SJ, et al. Natural biopolymers: novel templates for the synthesis of nanostructures. *Langmuir*. 2010;26:8497–8502.
16. Drogat N, Granet R, Sol V, et al. Antimicrobial silver nanoparticles generated on cellulose nanocrystals. *J Nanopart Res*. 2011;13:1557–1562.
17. Liu H, Song J, Shang SH, Song ZH, Wang D. Cellulose nanocrystal/silver nanoparticle composites as bifunctional nanofillers within waterborne polyurethane. *ACS Appl Mater Interfaces*. 2012;4:2413–2419.
18. Chandy T, Sharma, CP. Prostaglandin E1-immobilized poly(vinyl alcohol) blended chitosan membranes: blood compatibility and permeability properties. *J Appl Polym Sci*. 1992;44:2145–2156.
19. Park JS, Park JW, Ruckenstein E. Thermal and dynamic mechanical analysis of PVA/MC blend hydrogels. *Polymer*. 2001;42:4271–4280.
20. Lu BW, Chen WC. A disposable glucose biosensor based on drop-coating of screen-printed carbon electrodes with magnetic nanoparticles. *J Magn Magn Mater*. 2006;304:400–402.
21. Nakano Y, Bin Y, Bando M, et al. Structure and mechanical properties of chitosan/poly(vinyl alcohol) blend films. *Macromol Symp*. 2007;258:63–81.
22. Wang Q, Du YM, Fan LH. Properties of chitosan/poly(vinyl alcohol) films for drug-controlled release. *J Appl Polym Sci*. 2005;96:808–813.
23. Liang S, Liu L, Huang Q, Yam KL. Preparation of single or double-network chitosan/poly(vinyl alcohol) gel films through selectively cross-linking method. *Carbohydr Polym*. 2009;77:718–724.
24. Azizi S, Ahmad MB, Hussein MZ, Ibrahim NA. Synthesis, antibacterial and thermal studies of cellulose nanocrystal stabilized ZnO-Ag heterostructure nanoparticles. *Molecules*. 2013;18:6269–6280.
25. Costa-Júnior ES, Barbosa-Stancioli EF, Mansur AAP, Vasconcelos WL, Mansur HS. Preparation and characterization of chitosan/poly(vinyl alcohol) chemically crosslinked blends for biomedical applications. *Carbohydr Polym*. 2009;76:472–481.
26. Yamada M, Honma I. Anhydrous proton conductive membrane consisting of chitosan. *Electrochim Acta*. 2005;50:2837–2841.
27. Ebeling T, Paillet M, Borsali R, et al. Shear-induced orientation phenomena in suspensions of cellulose microcrystals, revealed by small angle X-ray scattering. *Langmuir*. 1999;15:6123–6126.
28. Rueda L, Saralegui A, Fernández d'Arlas B, et al. Cellulose nanocrystals/polyurethane nanocomposites. Study from the viewpoint of microphase separated structure. *Carbohydr Polym*. 2013;92:751–757.
29. Yi XX, Ying QY, Jiu YX, Shi FY, Wang F. Properties of novel polyvinyl alcohol/cellulose nanocrystals/silver nanoparticles blend membranes. *Carbohydr Polym*. 2013;98:1573–1577.
30. Khorsand ZA, Abrishami ME, Majid WHA, Yousefi R, Hosseini SM. Effects of annealing temperature on some structural and optical properties of ZnO nanoparticles prepared by a modified sol-gel combustion method. *Ceramics International*. 2011;37:393–398.
31. Azizi S, Ahmad MB, Namvar F, Mohamad R. Green biosynthesis and characterization of zinc oxide nanoparticles using brown marine macroalga Sargassum muticum aqueous extract. *Mater Lett*. 2014;116:275–277.
32. Mulvaney P. Surface plasmon spectroscopy of nanosized metal particles. *Langmuir*. 1996;12:788–800.
33. Xu JC, Liu WM, Li HL. Titanium dioxide doped polyaniline. *Mater Sci Eng C*. 2005;25:444–447.
34. Kannusamy P, Sivalingam T. Chitosan ZnO/polyaniline hybrid composites: polymerization of aniline with chitosan ZnO for better thermal and electrical property. *Polym Degrad Stabil*. 2013;98:988–996.
35. Kumar A, Vemula PK, Ajayan PM, John G. Silver-nanoparticle-embedded antimicrobial paints based on vegetable oil. *Nat Mater*. 2008;7:236–241.
36. Zhang J, Roll D, Geddes CD, Lakowicz JR. Aggregation of silver nanoparticle-dextran adducts with concanavalin A and competitive complexation with glucose. *J Phys Chem B*. 2004;108:12210–12214.
37. Wang XH, Du YM, Liu H. Preparation, characterization and antimicrobial activity of chitosan-Zn complex. *Carbohydr Polym*. 2004;56:21–26.
38. Qin YM, Zhu CJ, Chen J, Chen YZ, Zhang C. The absorption and release of silver and zinc ions by chitosan fibers. *J Appl Polym Sci*. 2006;101:766–771.
39. Kikuchi Y, Sunada K, Iyoda T, Hashimoto K, Fujishima A. Photocatalytic bactericidal effect of TiO_2 thin films: fynamic view of the active oxygen species responsible for the effect. *J Photochem Photobiol A Chem*. 1997;106:51–56.
40. Brayner R, Ferrari-Iliou R, Brivois N, Djediat S, Benedetti MF, Fiévet F. Toxicological impact studies based on *Escherichia coli* bacteria in ultrafine ZnO nanoparticles colloidal medium. *Nano Lett*. 2006;6:866–870.
41. Azizi S, Ahmad MB, Mahdavi M, Abdolmohammadi S. Preparation, characterization, and antimicrobial activities of ZnO nanoparticles/cellulose nanocrystal nanocomposites. *Bioresources*. 2013;8:1841–1851.